SOFT ROBOTICS Volume 00, Number 00, 2022 © Mary Ann Liebert, Inc. DOI: 10.1089/soro.2021.0065



Open camera or QR reader and scan code to access this article and other resources online.



Versatile Adhesion-Based Gripping via an Unstructured Variable Stiffness Membrane

Aoyi Luo, Sumukh S. Pande, and Kevin T. Turner

Abstract

Reversible and variable dry adhesion is a promising approach for versatile robotic grasping. Variable stiffness materials with a modulus that can be tuned using an external stimulus offer a unique approach to realize dynamic control of adhesion. In this study, an unstructured shape memory polymer (SMP) membrane with variable stiffness is used to pick-and-place three-dimensional objects. The variable stiffness of the SMP allows the membrane to conform to and make good contact with objects of various shapes in its soft state and then achieve high adhesive load capacity by switching to the stiff state. Release of objects is realized by switching to the soft state. The ratio between the high-adhesion and low-adhesion state is demonstrated to be >2000 on a curved substrate and ~ 115 on a flat substrate. This gripper exhibits no adhesion in the unactivated state and maintains adhesion passively once actuation is complete.

Keywords: dry adhesives, switchable adhesion, variable stiffness, robotic gripper

Introduction

Robots to grip and manipulate objects. Dry adhesion-based grippers that exploit van der Waals forces provide a promising alternative to friction-based grippers. Since dry adhesion prevents two contact surfaces from both sliding and separating, it can provide gripping forces that act both tangential and normal to the surface of an object. Microstructured and fibrillar adhesives have been the predominant approach to date for realizing strong and reversible dry adhesion. ¹⁻⁴ These adhesives have been most commonly applied to the pick-and-place of planar objects, yet adhesion to three-dimensional (3D) objects is critical in many applications.

Several dry adhesion-based grippers that allow for attachment to 3D objects have been reported. Hawkes *et al.*⁵ fabricated gecko inspired fibrillar adhesive films on a bistable

support structure and utilized the high shear force capacity of a fibrillar adhesive to grip 3D objects. Song and Sitti⁶ developed a device in which a gecko inspired fibrillar adhesive membrane was suspended above a chamber to allow the membrane to deform to accommodate to the shape of the object being contacted. Song *et al.*⁷ subsequently demonstrated that the force capacity of this device could be increased by applying a negative (i.e., vacuum) pressure on the membrane.

Although most of the dry adhesion-based grippers to date rely on gecko inspired structures, there are other routes to achieve strong dry adhesion. 8-10 It has been observed that the load capacity of an adhered interface scales with the square root of the product of system stiffness and contact area. 9,11 However, high system stiffness and large contact area generally cannot be achieved simultaneously, since compliance is essential for adhesives to reach large contact area.

Materials with variable stiffness, ^{12–14} which can switch between a stiff and a soft state in response to a specific stimulus, provide a unique opportunity to overcome this dilemma.

Shape memory polymers (SMPs) are a class of variable stiffness materials. ^{15–17} Bulk SMPs with unpatterned and micropatterned surfaces supported by a planar rigid backing have been used previously to grip macro- and microscale objects. ^{12,18–24} Other variable stiffness materials such as jammed granular materials, ^{25,26} foams, ²⁷ liquid metals, ¹³ wax, ²⁸ thermoplastics, ^{29,30} and hydrogels ¹⁴ have also been used in pick-and-place applications. Although SMP adhesives with various surface structures have been engineered to achieve strong and variable interfacial adhesion, the mechanical design of SMP adhesive systems with high compliance and conformability has received relatively little attention. The compliance and conformability of the previous studied SMP adhesives are limited by the planar rigid backing.

Membranes made of low modulus materials are highly effective at adapting to and conforming to nonplanar and deformable objects because of their low axial stiffness and negligible bending stiffness. ^{31,32}

In this study, we present a dry adhesion-based SMP gripper that exploits variable stiffness membrane for adhesion control (Fig. 1). The gripper is composed of an unstructured flat variable stiffness SMP membrane, which requires no microfabrication and can be manufactured using a simple casting process, supported on a pressure chamber that contains a heater. During use, the SMP membrane is heated, softens, and is then pressed in to contact with the target surface. The low modulus of the SMP in the soft state allows for conformal contact with complex surfaces. After making contact, the membrane is cooled and stiffens, resulting in increased load capacity. Release of the object is achieved by heating the membrane which softens the membrane and reduces the load capacity. Through the use of the unstructured variable stiffness SMP membrane design, the gripper can adapt to objects with varying 3D shapes, and achieve high load capacity and adhesion switching ratio compared to grippers based on elastomer membranes. 6,7,33

Materials and Methods

Fabrication of the SMP adhesive gripper

A cylindrical chamber with a 25.4 mm depth, 31.8 mm outer radius, and 28 mm inner radius was machined out of aluminum. The chamber has four 9.5 mm diameter holes, spaced 90° apart in the sidewall of the chamber for the air inlets and outlets, and an additional 6.4 mm diameter hole for the heater and the thermocouple wires. A thermocouple (SA1XL-K-72; Omega Engineering) was bonded to the backside of a 25.4 mm-radius 31 W circular flexible polyimide heater (KHRA-2/10; Omega Engineering) using silicone sealant (8661 Super Silicone Sealant; 3M). The heater and the thermocouple were connected to a proportional-integralderivative controller (CN32PT-330; Omega Engineering) to monitor and control the temperature. Four silicone foam pillars with height 25.4 mm and diameter 5 mm (McMaster-Carr) were bonded to the top of the chamber, and the heater was bonded to these pillars. The gap around the heater and thermocouple wires was sealed with silicone.

Four flexible tubes were connected to the chamber. Two of the tubes were connected to valves to regulate the pressure within and airflow through the chamber, and the other two tubes were connected to an air pump (102 W 6624.5 L/h flow rate; VIVOHOME; Amazon) or a syringe pump (Pump 11 Elite; Harvard Apparatus) depending on the required pressure. The unstructured flat SMP membrane (fabrication of the SMP membrane is detailed in Supplementary Material) was bonded to the open side of the chamber with the silicone sealant.

Adhesion tests

The SMP adhesive gripper was attached to a mounting block and then fixed in a standard universal testing machine (MTS Criterion Model 43) fitted with a 50 N load cell (MTS LSB.501).

Stiff-state pull-off test. The curved testing substrates were polymethyl methacrylate (PMMA) balls (TAP Plastics) with radii of 6.35, 12.7, and 25.4 mm. The balls were glued to holders and fixed in the testing machine. A picture of the adhesion test setup is shown in Supplementary Figure S6. In a stiff-state pull-off test, the SMP membrane was brought into contact with the curved substrate at 70°C at a rate of 0.2 mm/s to a prescribed preload (varied from 2 to 8 N). After stabilizing the contact for another 10 s, the heater was turned off and the pump was turned on for 4 min to cool the device. To eliminate the minor temperature increase due to the heat generated by the pump, the device was also allowed to sit for another 4 min. In the cases where the SMP membrane was cooled passively by the environment (unfilled markers at $F_{pre} = 2 \text{ N}$ in Fig. 2A), the device was simply allowed to sit for 10 min after the heater was turned off. After cooling, the device was pulled off at a rate of 0.01 mm/s. The maximum force recorded during pull-off in each test is denoted as the stiff-state pull-off force.

Stiff-state pull-off test against a flat substrate was conducted in a similar way and is detailed in Supplementary Material.

Soft-state pull-off test. In the soft-state pull-off tests against a curved substrate, the membrane was kept at 70°C using the controller throughout the test. The SMP membrane was brought into contact with the curved substrate at a rate of 0.2 mm/s to a preload of 5 N. After stabilizing the contact for another 10 s, the device was pulled off at a rate of 0.01 mm/s. The maximum force recorded in the pull-off step in each test is denoted as the soft-state pull-off force. Soft-state pull-off test against a flat substrate was conducted in a similar way and is detailed in Supplementary Material.

Results and Discussion

Design of the gripper

Figure 1A shows the design of the SMP adhesive gripper. An unstructured flat SMP membrane is supported on a rigid chamber (internal radius of 28 mm), which is connected to a system that controls the pressure and flow of air through the chamber. A flexible heater (radius 22.5 mm) supported by compliant pillars is in contact with the SMP membrane, and a thermocouple attached to the heater is used for measurement and control of the temperature. The unstructured flat SMP membrane is 1.6 mm thick and is made of a thermally responsive SMP (two-part epoxy, EPON 826 resin, Hexion, and

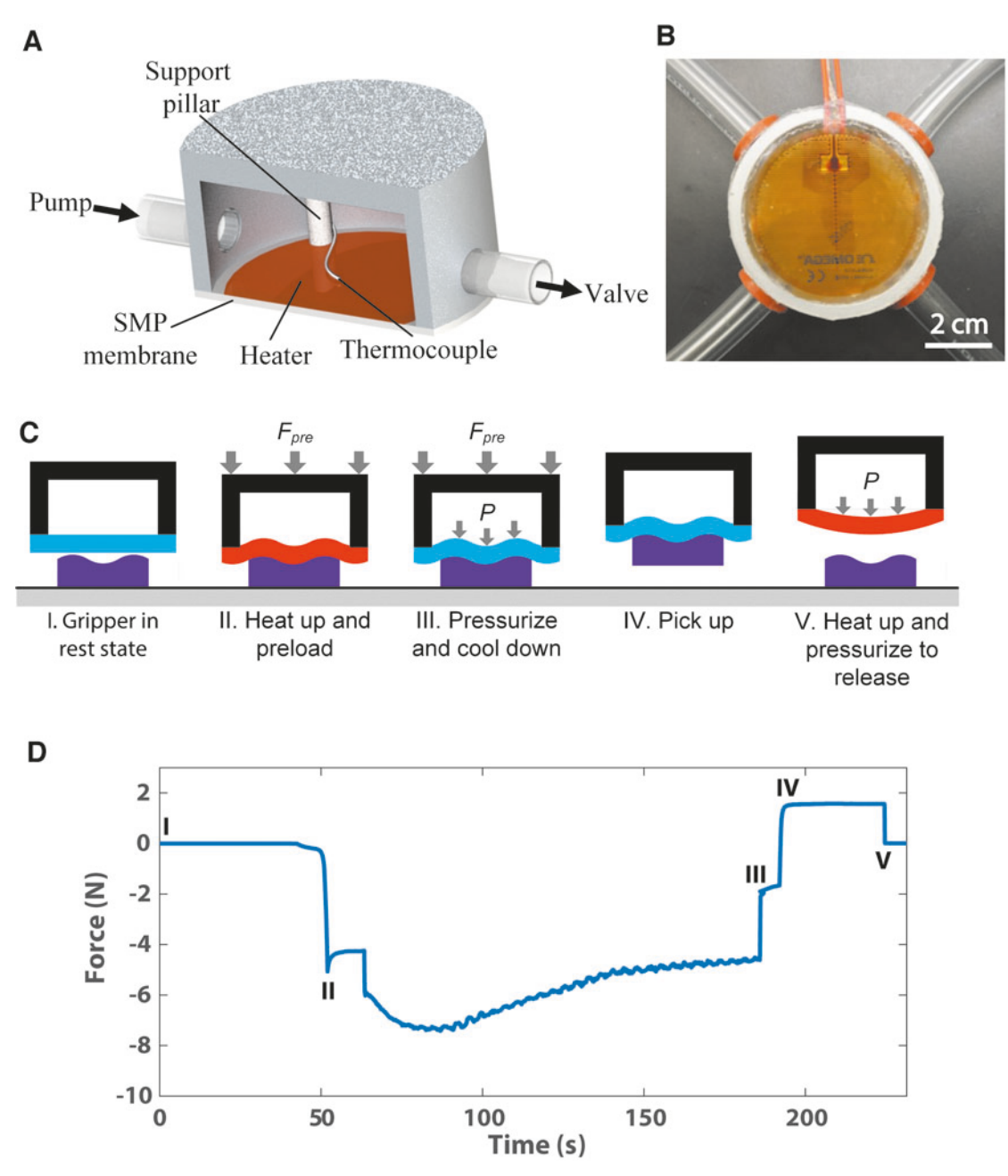


FIG. 1. Overview of the SMP adhesive end effector. (**A**) Schematic of the end effector showing the SMP membrane, support chamber, and heater. (**B**) A picture of the SMP adhesive end effector viewed from the membrane side. (**C**) Principle of operation of the SMP end effector for picking up and releasing an object. (**D**) A typical load versus time curve shown for the SMP end effector picking and releasing a 161 g PMMA sheet. The end effector in its rest state (I) was first heated to 70°C and contacted the object with a preload of 5 N (II); after waiting for 10 s, the heater was turned off, and an air pump was turned on for 120 s to convectively cool the SMP membrane and apply a 6.9 kPa pressure to the membrane (III); after the pump was turned off for 10 s, the object was picked up (IV) and held; then the heater was turned on again for 8 s, and the object was released (V). PMMA, polymethyl methacrylate; SMP, shape memory polymer.

Jeffamine D230 [poly(propylene glycol)bis (2-aminopropyl) ether] curing agent; Huntsman Corp.) with a transition temperature of $T_{\rm g}$ =60°C. ¹²

When heated sufficiently above the transition temperature $(T \ge 70^{\circ}\text{C})$, the SMP softens and the modulus is $E_r = 6.3 \text{ MPa}$. When sufficiently below the transition temperature (approximately $T \le 40^{\circ}\text{C}$), the SMP is in its stiff state with $E_c = 2.1 \text{ GPa}$. If held in a deformed state while cooling, the

deformed shape is locked in after the membrane is cooled below the transition temperature. ¹² This SMP has an excellent ability to both retain the deformed temporary shape after cooling and to recover the original permanent shape after being reheated above the transition temperature. ¹² The transition temperature can be tuned through the SMP formulation (i.e., mixing ratio of the epoxy monomer and the curing agent ¹²), and $T_{\rm g} = 60$ °C was chosen to avoid unintended

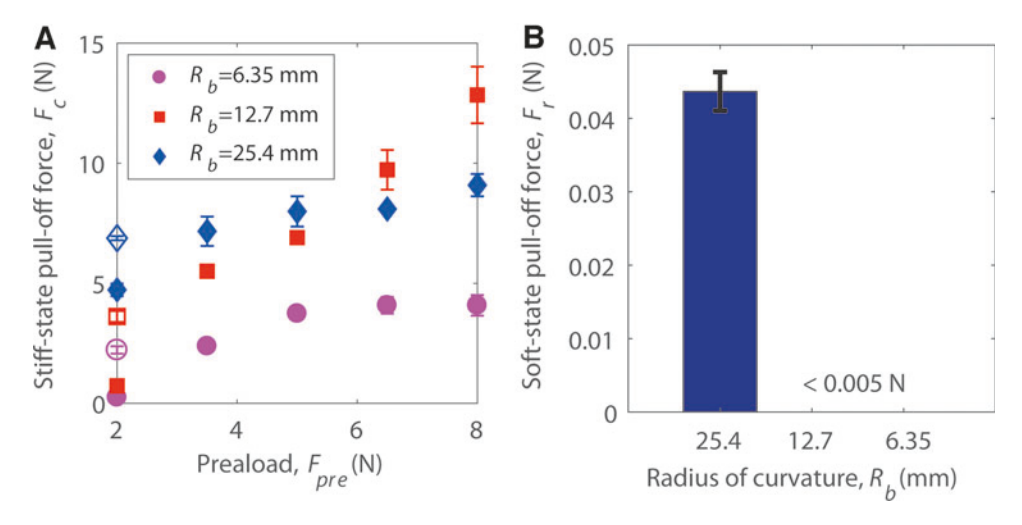


FIG. 2. Adhesion characterization of the SMP adhesive gripper. (**A**) The measured pull-off force in the stiff-state ($F_{\rm c}$) as a function of preload ($F_{\rm pre}$) for tests on curved PMMA substrates with $R_{\rm b}$ = 25.4, 12.7, 6.35 mm (open markers at $F_{\rm pre}$ = 2 N are stiff-state pull-off forces measured with the SMP membrane cooled passively by the environment to reduce vibration during cooling) (error bar denotes standard deviation of three tests). (**B**) Measured soft-state pull-off force ($F_{\rm r}$) on curved PMMA substrates with $R_{\rm b}$ = 25.4, 12.7, 6.35 mm.

actuation as it is higher than the temperatures of typical use environments but also sufficiently low to allow for relatively fast heating to the transition temperature.

A picture of the gripper (Fig. 1B) shows the transparent unstructured flat SMP membrane bonded to an aluminum chamber and a flexible polyimide heater in contact with the backside of the membrane. Four tubes are connected to the chamber, two of which are connected to a pump and the other two are connected to valves that vent to atmosphere when open. A total of four ports, rather than the minimum of two, are used to provide a more uniform airflow over the SMP membrane during cooling to enhance convection.

Principle of operation

Figure 1C illustrates the principle of operation of the SMP adhesive gripper, and Figure 1D shows a typical load versus time curve for pick-and-place of a 161-g PMMA sheet. When not heated, the SMP membrane is stiff and cannot easily make conformal contact with other surfaces (Fig. 1C—I), thus preventing unintentional adhesion. During use, the SMP membrane is heated to 70°C to soften the SMP, which takes 29 s, and then the membrane is contacted to the object (Fig. 1C—II). The contact is formed by displacing the chamber supporting the SMP membrane to bring the membrane into contact with the object. In addition, in some cases, such as for contacting nonconvex objects, the chamber can be pressurized to apply a preload over the entire membrane. While maintaining the contact, the SMP membrane is cooled to 30°C by turning the heater off and flowing air through the chamber which takes 89 s (Fig. 1C—III). Upon cooling and stiffening, higher load capacity is realized, allowing gripping of various objects (Fig. 1C—IV). Importantly, no power is needed for the gripper to maintain this gripping state.

Objects are released through heating and softening of the SMP membrane (Fig. 1C—V). The load capacity decreases with softening of the membrane, and detachment is also facilitated by the tendency for the SMP to return to its orig-

inal shape when heated. Pressure can also be applied during the release process to deform the contact and further reduce the adhesion.

Adhesion characterization

The ability of an adhesion-based gripper to pick up an object depends on its adhesive force capacity, and this is characterized by measuring the pull-off force of the gripper with the SMP in the stiff state. Measurements were performed against curved PMMA substrates with three different radii of curvatures, R_b. The stiff-state pull-off test was conducted by first heating the SMP membrane to its soft state and bringing the membrane into contact with the substrate at a given preload, then cooling to 30°C to stiffen the membrane, and subsequently displacing the gripper away from the substrate at 0.01 mm/s until pull-off occurs. The slow displacement rate is used to minimize the effect of viscoelasticity (for completeness, the effect of the displacement rate on the stiffstate pull-off force is shown in Supplementary Fig. S1A). The maximum force measured during the pull-off process is denoted as the stiff-state force capacity, F_c .

The measured stiff-state force capacity as a function of preload and substrate curvature is shown in Figure 2A. Higher adhesion was achieved with higher preload for all the curved substrates tested—this is different from conventional dry adhesives composed of materials with no shape memory effect where the adhesion reaches a plateau at a critical preload value. ^{6,7} For a material without the shape memory effect, increasing the preload increases the contact area but it also increases the stored elastic energy that counteracts adhesion. However, in the case of the SMP, the deformed shape in the preload step is locked in after cooling and the contact area is maintained. As a result, the adhesive force capacity increases with increasing preload when gripping a 3D object such as a curved substrate.

Based on the same argument, the SMP is expected to maintain higher adhesion performance compared to other adhesives made of materials that have comparable soft state modulus but without shape memory effect when the surfaces are slightly damaged (e.g., scratched). This is because a slightly damaged SMP surface can still be heated and preloaded to achieve contact with the object and fix the contact after cooling, while a slightly damaged nonshape memory material surface that is preloaded into contact with an object will have an increased elastic energy penalty.

Generally, for a given preload, higher adhesion is expected on substrates that are flatter, that is, substrates with larger radii of curvature. This trend holds for the SMP gripper when the preload is small ($F_{\text{pre}} \le 5 \text{ N}$); however, for larger preload ($F_{pre} > 5 \text{ N}$), the adhesion on a curved substrate with $R_b = 12.7 \text{ mm}$ is higher than that on a curved substrate with $R_b = 25.4 \,\mathrm{mm}$ (Fig. 2A). The underperformance of the SMP adhesive gripper on the curved substrate with $R_b = 25.4$ mm at a large preload is believed to be caused by nonuniform heating of the SMP membrane. The heater has an effective heating radius of 22.5 mm, so it is expected that only the center portion of the SMP membrane is heated sufficiently to its soft state to make conformal contact. As a result, the contact area and the adhesion achieved at a high preload on the curved substrate with $R_b = 25.4 \,\mathrm{mm}$ may be smaller compared to the case where the membrane is uniformly heated throughout.

It was observed that for small preloads ($F_{pre} = 2 \,\mathrm{N}$), the oscillation of the airflow generated by the pump during cooling can deteriorate the quality of the contact and reduce the adhesion. The adhesion in the absence of vibration of the membrane was characterized by cooling the SMP membrane passively by the environment, and the corresponding pull-off forces are included as open markers in Figure 2A. The absence of vibration during cooling increases the adhesion at small preloads for all the curved substrates tested, but there is no discernible difference in the adhesion obtained between the two cases when the preload is larger ($F_{pre} > 2 \text{ N}$). This could potentially be an issue for pick-and-place of fragile objects where only a small preload can be applied but could be overcome by improving the uniformity of the flow, for example, using a compressed air reservoir or a fan rather than a mechanical pump.

A successful pick-and-place operation also requires the ability to release objects. The performance of the gripper on this metric is characterized using soft-state pull-off tests against the same curved PMMA substrates. In the soft-state pull-off tests, the SMP membrane is heated up to its soft state and brought into contact with the substrate, then pulled off at a speed of 0.01 mm/s while the temperature is maintained (effect of the pull-off speed on the soft-state pull-off force is shown in Supplementary Fig. S1B). The measured soft-state pull-off force F_r , which is the maximum force obtained during the soft-state pull-off process, quantitatively describes the ability of the SMP adhesive gripper to release an object and a smaller force is more favorable.

The soft-state pull-off forces, shown in Figure 2B, are independent of preload. The soft-state pull-off force is $\sim 0.045 \,\mathrm{N}$ on the curved substrate with $R_{\rm b} = 25.4 \,\mathrm{mm}$ and is $< 0.005 \,\mathrm{N}$ (less than the noise floor of the force sensor) on the curved substrates with $R_{\rm b} = 12.7$ and 6.35 mm. Thus, the adhesion switching ratio (the ratio of the stiff-state pull-off force to the soft-state pull-off force) is ~ 200 on the $R_{\rm b} = 25.4 \,\mathrm{mm}$ substrate and $> 2000 \,\mathrm{and} > 600$ on the $R_{\rm b} = 12.7$ and 6.35 mm substrates, respectively.

Analytical modeling

To understand the effect of different design parameters, notably geometry and material properties, on the adhesion of the device, a simple analytical membrane model (which ignores bending deformation), adapted from Song et al., 7,34 that estimates the adhesion of the device to a curved substrate was developed. The model is based on idealized assumptions that are not fully satisfied in the experiment: The SMP is uniformly heated to its soft state and completely recovers the original permanent shape after being heated to the soft state; it completely fixes the deformed temporary shape after being cooled to the stiff state. Details of the model are presented in the Supplementary Material (Supplementary Fig. S2), and the results are summarized in Supplementary Figures S3–S5. From Supplementary Figure S4, the calculated stiff-state pull-off force on a curved substrate using this model is found to scale with the square root of the preload F_{pre} , work of adhesion G_c , modulus switching ratio E_c/E_r , and radius of curvature of the substrate $R_{\rm b}$ over the range of parameters investigated:

$$F_{\rm c} \propto \sqrt{F_{\rm pre}G_{\rm c}\frac{E_{\rm c}}{E_{\rm r}}R_{\rm b}}.$$
 (1)

The calculated stiff-state pull-off force is positively correlated to the modulus switching ratio $E_{\rm c}/E_{\rm r}$ because of two effects: (1) a higher stiff-state modulus $E_{\rm c}$ leads to a higher stiff-state pull-off force because it reduces system compliance, (2) a lower soft-state modulus $E_{\rm r}$ increases the contact radius achieved during the preload step. Membrane thickness h is absent from Equation (1) because while a larger membrane thickness reduces compliance and increases the stiff-state pull-off force, the larger membrane thickness also reduces the contact radius achieved during preloading. The pull-off force on a curved substrate in the soft state is found to scale with the work of adhesion $G_{\rm c}$ and radius of curvature of the substrate $R_{\rm b}$ as shown in Supplementary Figure S5 and is relatively insensitive to other parameters over the range investigated:

$$F_{\rm r} \propto G_{\rm c} R_{\rm b}$$
. (2)

The soft-state pull-off force is insensitive to membrane thickness h and soft-state modulus $E_{\rm r}$. A larger membrane thickness h or a larger soft-state modulus $E_{\rm r}$ leads to a higher membrane stiffness. While a higher membrane stiffness improves the load sharing, it also increases the elastic energy penalty when conforming to a nonplanar surface. The same trend was noted by Song $et\ al.^{35}$

While both the calculated stiff-state and soft-state pull-off forces are not affected by the thickness of the membrane h and the soft-state modulus E_r (for a fixed modulus switching ratio E_c/E_r), thinner membranes and materials with lower soft state modulus E_r result in more compliant membranes in the soft state and thus can achieve larger contact areas. Within the assumptions of the model, a larger contact area is predicted during the preload step, Supplementary Figure S3, which improves gripping stability (e.g., improved ability to resist moments applied to the contact and off-axis loads). Beyond the membrane-level deformations considered in the model, a lower stiffness membrane also allows better local

conformal contact. This results in an improved ability to grasp objects with complex geometries and also may yield higher effective $G_{\rm c}$ through improved accommodation of roughness. ³⁶

Effect of pressure on adhesion

Application of pressure inside the chamber in different steps of the operation provides the opportunity to enhance the performance of the gripper. Application of a positive pressure during the preload step can improve the contact area, while applying a negative pressure during the stiff-state pull-off step can increase the load capacity. Furthermore, maintaining a positive pressure during the soft-state pull-off step can reduce the adhesion and allow for object release at lower loads. These benefits are demonstrated through pull-off tests against a flat PMMA substrate.

If the preload step is conducted simply by displacing the SMP membrane against the flat substrate, the compressive preload is primarily concentrated around the edge of the SMP membrane through the chamber wall, leaving the central region of the membrane largely unloaded. This nonuniform preload, as well as possible misalignment and surface roughness of both surfaces, limits contact of the membrane and leads to a stiff-state pull-off force of only 0.9 N for a flat substrate (denoted as "Press" in Fig. 3A). However, a positive pressure applied after the membrane is displaced to contact the substrate during the preload step results in better contact across the full SMP membrane, for example, application of 6.9 kPa pressure in the preload step increases the stiff-state pull-off force to 10.9 N (denoted as "6.9 kPa preload" in Fig. 3A). The application of a positive pressure during preload is especially beneficial for achieving large contact area to nonconvex objects.

Moreover, a negative pressure can be applied during the stiff-state pull-off step to increase the load capacity, similar to Song *et al.*⁷ After the contact was formed by applying 6.9 kPa pressure in the preload step, the membrane was cooled to its stiff state and then pulled off with a negative pressure of magnitude 6.9 kPa. The negative pressure resulted in a load capacity of 21.2 N ("-6.9 kPa pull-off" data in Fig. 3A). The increased load capacity due to the applied negative pressure is primarily due to improved load sharing across the membrane, similar to that reported by Song *et al.*⁷ In addition, there is a potential contribution to the adhesion from suction as noted by Song *et al.*³⁷

Finally, we demonstrate that soft-state pull-off force can be decreased through application of a positive pressure during release. A decrease in pull-off force with positive pressure is expected for the blister configuration based on previous work.^{6,38} In a soft-state pull-off test against the flat substrate, the same contact as that in the stiff-state pull-off test was first generated by applying 6.9 kPa pressure in the preload step, then different positive pressures were applied during the softstate pull-off step to investigate the effect of pressure on the soft-state pull-off force. The results, summarized in Figure 3B, show that the soft state adhesion is significantly reduced when a positive pressure is applied. While the adhesion is expected to monotonically reduce with increasing pressure for a blister configuration, 6,38 the pull-off force observed in experiments increased slightly at the highest pressure (4.8 kPa in Fig. 3B). This is likely due to the membrane being deformed farther from the heater at high applied pressures resulting in some cooling and hence stiffening of the membrane.

Figure 3C summarizes the adhesion switching ratio (F_c/F_r) on the flat substrate as a function of the stiff-state pull-off test operation procedures (operation procedures "Press," "6.9 kPa preload," and "-6.9 kPa pull-off" are described

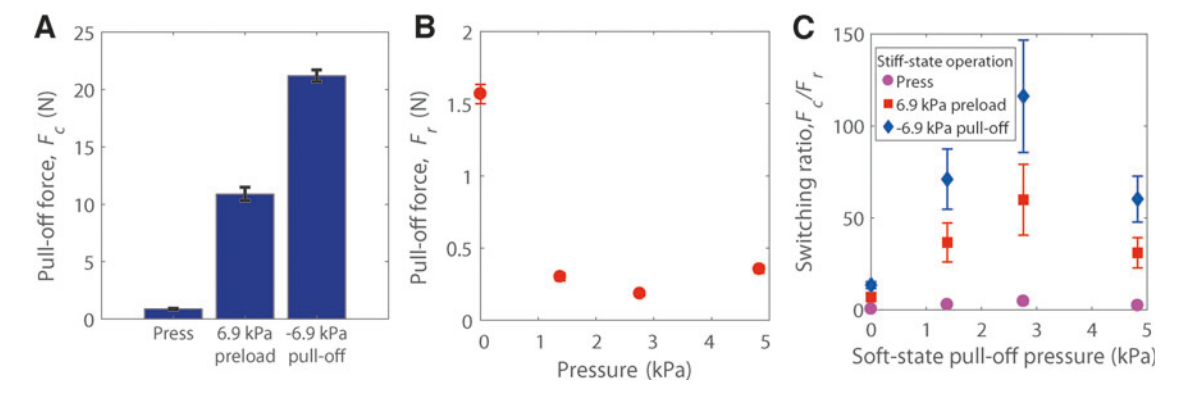


FIG. 3. Use of pressure to enhance SMP adhesive end effector performance. (**A**) Measured stiff-state pull-off forces (F_c) on a flat PMMA substrate for different operation procedures: Press: (i) the SMP membrane is heated to the soft state and displaced against the substrate to form contact with no pressure applied in the chamber, (ii) cooled to the stiff state and pulled off; 6.9 kPa presoure is applied inside the chamber to improve the contact between the membrane and surface, (iii) cooled to the stiff state and pulled off after removing the 6.9 kPa pressure; -6.9 kPa pull-off: (i) the SMP membrane is heated to the soft state and displaced against the substrate to form contact, (ii) 6.9 kPa pressure is applied inside the chamber to enhance contact, (iii) cooled to the stiff state and pulled off with the -6.9 kPa pressure maintained inside the chamber (error bar denotes standard deviation of three tests). (**B**) Measured soft-state pull-off force (F_r) on a flat PMMA substrate with different pressures inside the chamber (error bar denotes standard deviation of three tests). (**C**) Adhesion switching ratio (F_c/F_r) on a flat PMMA substrate as a function of the stiff-state pull-off test operation procedures ("Press," "6.9 kPa preload," and "-6.9 kPa pull-off" shown in **A**) and the applied pressure during soft-state pull-off test (shown in **B**).

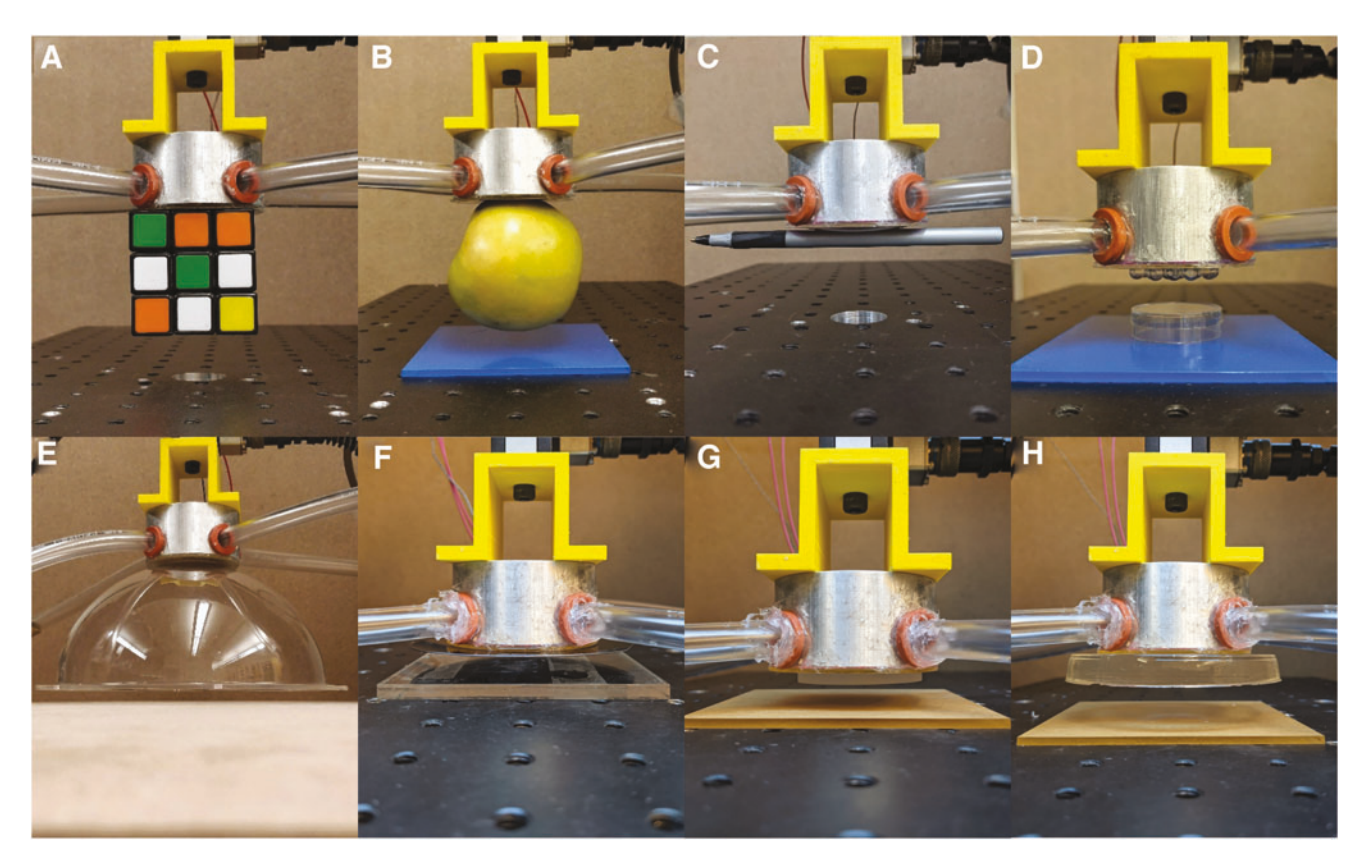


FIG. 4. Examples of the SMP adhesive gripper gripping various objects. (**A**) A 105-g Rubik's CubeTM. (**B**) A 150-g apple. (**C**) A 4-g pen. (**D**) An array of 24 individual 6.35 mm diameter 0.16-g plastic beads. (**E**) A 116-g plastic dome with a radius of curvature of 90 mm. (**F**) A 10-g silicon wafer. (**G**) A 14-g double concave lens with diameter 50 mm and focal length 200 mm. (**H**) A 61-g polydimethylsiloxane block.

above and in the caption of Fig. 3, and the corresponding data are shown in Fig. 3A) and the applied pressure during soft-state pull-off test (data shown in Fig. 3B), and a maximum adhesion switching ratio ~ 115 is achieved on a flat substrate.

Demonstrations

Finally, to demonstrate the gripping ability of the SMP adhesive gripper, the use of the SMP adhesive gripper to grip various 3D objects, including convex objects (Fig. 4B, C, D, E), flat objects (Fig. 4A, F), a concave object (Fig. 4G), and a deformable object (Fig. 4H), is highlighted in Figure 4 (syringe pump was used to pressurize the contact with the double concave lens to avoid fluctuation created by the air pump; Fig. 4G). All the objects are easily released when the SMP membrane is heated (6.9 kPa pressure was applied in addition to heating to facilitate the release of the 0.16 plastic beads; Fig. 4D). Supplementary Videos S1 to S3 show the SMP adhesive gripper pick-and-place of a 10-g silicon wafer, a 61-g polydimethylsiloxane block and a 14-g double concave lens.

Limitations

While the versatility of the SMP gripper was demonstrated, there are aspects that should be advanced in future work. Two key areas for improvement are the response time and energy consumption of the gripper. Heating of the SMP membrane was done using a heater placed close to the membrane, requiring 29 s and 899 J to heat the SMP membrane from 19°C to 70°C (thermal characterization is detailed

in Supplementary Material). A heater integrated directly on the membrane would allow for faster and more uniform heating and reduce the heat loss due to contact resistance between the heater and the membrane. This could be realized by integrating a stretchable heater directly on the membrane using existing techniques. 31,39,40

Compared to heating, cooling generally provides a more significant constraint on the response time of thermally actuated devices. ^{7,23,41} In the current device, when the membrane is cooled passively through heat conduction, it takes \sim 290 s for the membrane to cool from 70°C to 30°C. Flowing air through the chamber at ~ 1.8 L/s reduces the cooling time by more than 3× to 87 s, while introduction of the convection required an additional 8874 J of energy (note: this is the energy consumption of the pump used for cooling in the demonstration experiment; importantly, this pump was not selected based on energy efficiency and a more efficient source for creating air flow could be used). We note that the high surface area to volume of the membrane geometry requires less energy consumption for heating for a given available contact area and allows for faster cooling through convection compared to other thermally actuated devices. ^{19,23,28,30} The cooling rate of the device and its cooling energy consumption could be further improved by using a thinner membrane or miniaturizing the device or introducing more efficient forced convection.

Another limitation of this dry adhesion-based device is that it is primarily designed to pick-and-place of objects with smooth surfaces just as many other dry-adhesion based devices^{5–7} and fails to adhere to surfaces with large amplitude

fine-scale roughness (e.g., a frosted acrylic sheet), although its adhesion to rough surfaces could be potentially enhanced using a different SMP with a lower soft-state modulus to improve conformability to rough surfaces.

Conclusion

We have demonstrated and characterized a SMP adhesive gripper that exploits variable stiffness to controllably pick-and-place 3D objects. This device is composed of an unstructured variable stiffness SMP membrane bonded to a chamber that can be pressurized. The SMP membrane is heated to its soft state and conforms to the object upon contact under preload. Upon cooling to its stiff state, the contact area achieved during preloading is maintained, while the adhesive load capacity is increased due to the increased modulus of the SMP. Note that in the stiff, high-adhesion state, the SMP is not heated, and thus, no power is needed to maintain the attachment.

Objects are released by heating the membrane to its soft state, which allows the interface to detach at comparatively low loads. The SMP adhesive gripper was demonstrated to have a load capacity of ~ 13 N and a switching ratio of >2000 on a curved substrate with a radius of curvature of 12.7 mm and a load capacity of ~ 21 N and a switching ratio of ~ 115 on a flat substrate. The ability to pressurize the chamber allows a preload to be applied across the membrane surface to make contact to flat and concave surfaces. Furthermore, pressurization can be used to increase the load capacity and facilitate release. While friction-based grippers cannot pick up planar objects and most dry adhesives only work well on planar objects, the adhesion-based gripper proposed here can grip a variety of 3D objects.

Acknowledgments

The authors thank Yuchen Guo for help in preparing for the experiments and thank Christopher Stabile for providing helpful comments on the article.

Authors' Contributions

A.L. conceptualized the idea, designed and fabricated the device, characterized the device, developed the model, and wrote and revised the article. S.S.P characterized the device and wrote the article. K.T.T. conceptualized the idea, supervised the research, and reviewed and revised the article.

Author Disclosure Statement

An invention disclosure report on the work in this article has been filed with the University of Pennsylvania. The University may decide to file a patent on parts of the work contained in this article.

Funding Information

This work was supported by the National Science Foundation under award 1830475 and 1663037.

Supplementary Material

Supplementary Data Supplementary Video S1 Supplementary Video S2 Supplementary Video S3

References

- Hensel R, Moh K, Arzt E. Engineering micropatterned dry adhesives: from contact theory to handling applications. Adv Funct Mater 2018;28:1800865.
- Del Campo A, Greiner C, Álvarez I, et al. Patterned surfaces with pillars with controlled 3D tip geometry mimicking bioattachment devices. Adv Mater 2007;19:1973–1977.
- 3. Murphy MP, Aksak B, Sitti M. Gecko-inspired directional and controllable adhesion. Small 2009;5:170–175.
- Xue L, Sanz B, Luo A, et al. Hybrid surface patterns mimicking the design of the adhesive toe pad of tree frog. ACS Nano 2017;11:9711–9719.
- Hawkes EW, Christensen DL, Han AK, et al. Grasping without squeezing: shear adhesion gripper with fibrillar thin film. Proc IEEE Int Conf Robot Autom 2015;2015:2305– 2312.
- Song S, Sitti M. Soft grippers using micro-fibrillar adhesives for transfer printing. Adv Mater 2014;26:4901

 –4906.
- Song S, Drotlef DiM, Majidi C, et al. Controllable load sharing for soft adhesive interfaces on three-dimensional surfaces. Proc Natl Acad Sci U S A 2017;114:E4344– E4353.
- Minsky HK, Turner KT. Achieving enhanced and tunable adhesion via composite posts. Appl Phys Lett 2015;106: 201604.
- Bartlett MD, Croll AB, King DR, et al. Looking beyond fibrillar features to scale gecko-like adhesion. Adv Mater 2012;24:1078–1083.
- Luo A, Mohammadi Nasab A, Tatari M, et al. Adhesion of flat-ended pillars with non-circular contacts. Soft Matter 2020;16:9534–9542.
- 11. Kendall K. An adhesion paradox. J Adhesion 1973;5:77–79.
- Eisenhaure J, Kim S. High-strain shape memory polymers as practical dry adhesives. Int J Adhes Adhes 2018;81:74– 78
- 13. Ye Z, Lum GZ, Song S, *et al.* Phase change of gallium enables highly reversible and switchable adhesion. Adv Mater 2016;28:5088–5092.
- 14. Cho H, Wu G, Jolly JC, *et al.* Intrinsically reversible superglues via shape adaptation inspired by snail epiphragm. Proc Natl Acad Sci U S A 2019;116:13774–13779.
- 15. Xie T. Tunable polymer multi-shape memory effect. Nature 2010;464:267–270.
- Miao W, Zou W, Jin B, et al. On demand shape memory polymer via light regulated topological defects in a dynamic covalent network. Nat Commun 2020;11:4257.
- Lendlein A, Jiang H, Jünger O, et al. Light-induced shapememory polymers. Nature 2005;434:879–882.
- 18. Eisenhaure JD, Xie T, Varghese S, *et al.* Microstructured shape memory polymer surfaces with reversible dry adhesion. ACS Appl Mater Interfaces 2013;5:7714–7717.
- 19. Linghu C, Zhang S, Wang C, *et al.* Universal SMP gripper with massive and selective capabilities for multiscaled, arbitrarily shaped objects. Sci Adv 2020;6:1–12.
- Seo J, Eisenhaure J, Kim S. Micro-wedge array surface of a shape memory polymer as a reversible dry adhesive. Extreme Mech Lett 2016;9:207–214.
- Eisenhaure JD, Rhee S II, Al-Okaily AM, et al. The use of shape memory polymers for MEMS assembly. J Microelectromech Syst 2016;25:69–77.
- 22. Huang Y, Zheng N, Cheng Z, *et al.* Direct laser writing-based programmable transfer printing via bioinspired shape

- memory reversible adhesive. ACS Appl Mater Interfaces 2016:8:35628-35633.
- Tan D, Wang X, Liu Q, et al. Switchable adhesion of micropillar adhesive on rough surfaces. Small 2019;15: 1904248.
- 24. Kim S, Sitti M, Xie T, *et al.* Reversible dry micro-fibrillar adhesives with thermally controllable adhesion. Soft Matter 2009;5:3689–3693.
- 25. Brown E, Rodenberg N, Amend J, *et al.* Universal robotic gripper based on the jamming of granular material. Proc Natl Acad Sci U S A 2010;107:18809–18814.
- Li L, Liu Z, Zhou M, et al. Flexible adhesion control by modulating backing stiffness based on jamming of granular materials. Smart Mater Struct 2019;28:115023.
- Swift MD, Haverkamp CB, Stabile CJ, et al. Active membranes on rigidity tunable foundations for programmable, rapidly switchable adhesion. Adv Mater Technol 2020;5:2000676.
- 28. Krahn J, Sameoto D, Menon C. Controllable biomimetic adhesion using embedded phase change material. Smart Mater Struct 2011;20:1–8.
- Tatari M, Mohammadi Nasab A, Turner KT, et al. Dynamically tunable dry adhesion via subsurface stiffness modulation. Adv Mater Interfaces 2018;5:1800321.
- 30. Coulson R, Stabile CJ, Turner KT, *et al.* Versatile soft robot gripper enabled by stiffness and adhesion tuning via thermoplastic composite. Soft Robot 2021;00:1–12.
- 31. Kim DH, Lu N, Ma R, *et al.* Epidermal electronics. Science 2011;333:838–843.
- 32. Peng Z, Chen S. Peeling behavior of a thin-film on a corrugated surface. Int J Solids Struct 2015;60:60–65.
- Arul EP, Ghatak A. Control of adhesion via internally pressurized subsurface microchannels. Langmuir 2012;28: 4339–4345.

- Song S, Majidi C, Sitti M. GeckoGripper: a soft, inflatable robotic gripper using gecko-inspired elastomer micro-fiber adhesives. IEEE Int Conf Intell Robots Syst 2014;4624

 4629.
- 35. Song S, Drotlef DM, Paik J, *et al.* Mechanics of a pressure-controlled adhesive membrane for soft robotic gripping on curved surfaces. Extreme Mech Lett 2019;30:100485.
- 36. Persson BNJ, Scaraggi M. Theory of adhesion: role of surface roughness. J Chem Phys 2014;141:124701.
- 37. Song S, Drotlef DM, Son D, *et al.* Adaptive self-sealing suction-based soft robotic gripper. Adv Sci 2021;8:2100641.
- Carlson A, Wang S, Elvikis P, et al. Active, programmable elastomeric surfaces with tunable adhesion for deterministic assembly by transfer printing. Adv Funct Mater 2012; 22:4476–4484.
- 39. Zhao R, Lin S, Yuk H, et al. Kirigami enhances film adhesion. Soft Matter 2018;14:2515–2525.
- 40. Markvicka EJ, Bartlett MD, Huang X, *et al.* An autonomously electrically self-healing liquid metal-elastomer composite for robust soft-matter robotics and electronics. Nat Mater 2018;17:618–624.
- 41. Shintake J, Cacucciolo V, Floreano D, *et al.* Soft robotic grippers. Adv Mater 2018;30:1707035.

Address correspondence to:

Kevin T. Turner

Department of Mechanical Engineering

and Applied Mechanics

University of Pennsylvania

220 South 33rd Street

Philadelphia, PA 19104-6315

USA

E-mail: kturner@seas.upenn.edu